GROUND BASED SKY DOME PICTURES GENERATED BY INFRARED SPECTROMETRIC DATA.

Thierry Besnard [1, 3], Didier Gillotay [*2], Laurent Berger [3], Fabrice Zanghi [4]
and Yvan Labaye [3].

(1) Groupe Leader, 76056 Le Havre, France.
(2) Institut d'Aéronomie Spatiale de Belgique, 1180 Bruxelles, Belgique.
(3) LPEC-CNRS UMR 6087, Université du Maine, 72085 Le Mans cedex 9, France.
(4) Météo-France, DSO/DOS, 7 rue Teisserenc de Bort,78041 Trappes France

1. INTRODUCTION

Through several communications (Gillotay et al.; Besnard et al.), we showed the evolution of "Nephelo project", relative to the design of an infrared cloud cover imager, from the basic idea up to the comparison with other sky imaging techniques and cloud cover intensity measurement methods. Before approaching experimentally physical properties of clouds by the integration of "water vapor sensors" in Nephelo, it appeared necessary to determine with a relative accuracy, the shape, orientation and position of clouds on the sky dome. In order to approach phenomenon progressively we decided to go through a 2D modelling process.

2. MODEL DESIGN

2.1 Measurement grid

Measurement grid of Nephelo is calculated by means of a parallel plan model. The grid is defined as the intersection between the field of view of each sensor and a plan at a defined altitude. Figure 1 shows this grid at 3000 m high. The X-axis gives the footprint distance along the South-North axis and the Y-axis the footprint distance along the West-East axis.

2.2 Virtual cloud definition

The shape of the most current types of clouds except cirrus can be approximate by an ellipse. Since the beginning of this program, experiments

---

* Corresponding author address: Dr. Didier Gillotay, Institut d'Aéronomie Spatiale de Belgique, 3 Avenue Circulaire, B-1180 Brussels, Belgium. dgill@oma.be
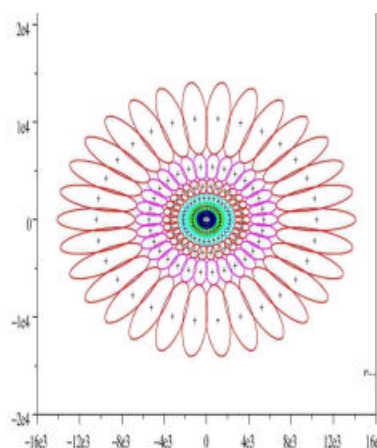
Figure 1: *Present grid of measurement of Nephelo.*

have demonstrated the fact that each Nephelo pyrometer measures the mean temperature of its integrated field of view on the sky dome, i.e. temperature of deep space and/or temperature of clouds. In the ellipse representing the virtual cloud, we considered that the emissivity is constant and equal to that of a black body.

This virtual cloud can move at a constant speed along the main axis of the ellipse during the Nephelo turret scan.

2.3 Surface intersection between virtual cloud and measurement ellipse.

The surface intersection between virtual cloud and each sensor ellipse is calculated following Monte Carlo method.

Figure 2 and 3 show that the criteria of quality of the random number generator in terms of distribution homogeneity and independence are well respected.

The method generates random sets of x and y values scaled properly to the size of the "shooting box". We check for each point if it is included in the virtual cloud ellipse and also in

one of the Nephelo ellipses. If points respect both criteria, they are used for calculation of the intersection surface. We run the Monte Carlo process (10^6 runs) when ellipses have an intersection determined by common x and y values.
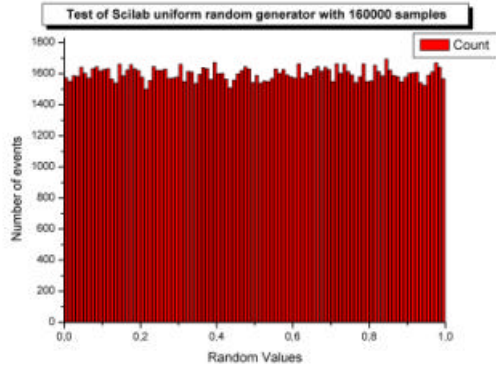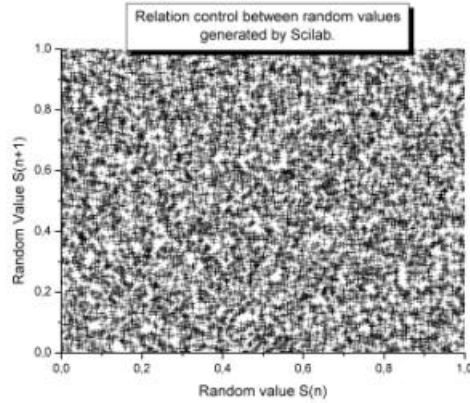

Figure 2: *Homogeneity of the random generator.*

Figure 3: *Independence of the random generator.*

The temperature of each Nephelo ellipse is determined with the following equation:

$$T_{nephelo} = A \times T_{virtual\ cloud} + (1-A) \times T_{background} \qquad (1)$$

where A is the surface percentage of the Nephelo ellipse covered by the virtual cloud ellipse and $T_{background}$ defined as the minimal temperature value ranged by used pyrometers; in our experimental conditions $T_{background}$ is initially set to –57°C.

3 FIRST SIMULATIONS

For this first batch of simulation we placed at the origin of the referential an elliptic virtual cloud with its main axis along the x'ox axis. Parameters of this ellipse are the following:

- a=3 km
- b=0.5 km
- CCW rotation angle=0°

Main characteristics of the different tests performed and thermal footprints are summarized in table 1.

Test	Altitude (m)	Temperature (°C)	Figure
1	10000	-43.1	
2	8000	-32.5	4
3	6000	-19	
4	4000	-4.5	
5	2000	8.3	5
6	1000	13	
7	500	14.7	

Table1

Temperature simulations are determined with MSISE-90 model for July 15th in Brussels (50°48'N-4°21'E).

Thermal footprints shown in figures 4 and 5 are obtained with a standard interpolation method. Irregularities are due to a lack of resolution.
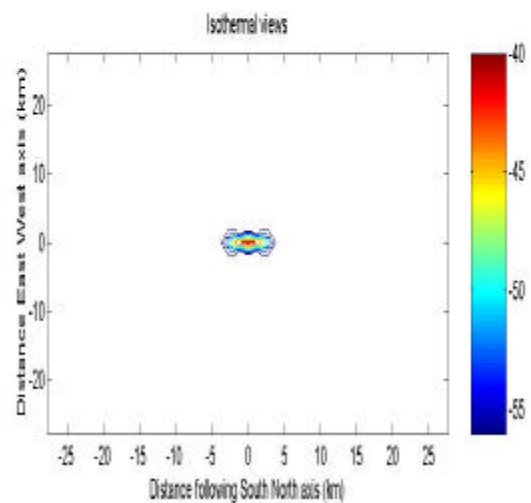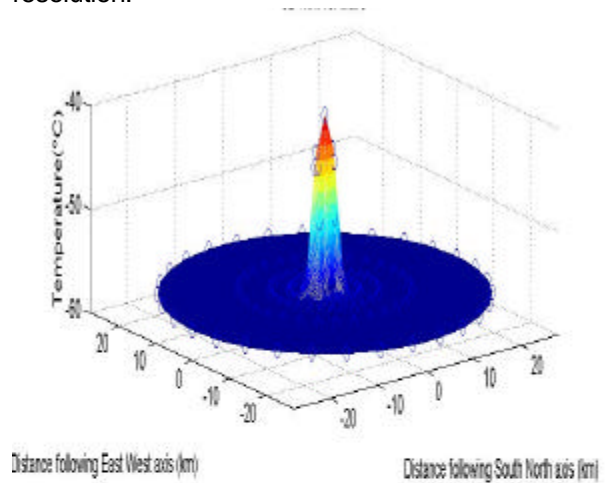

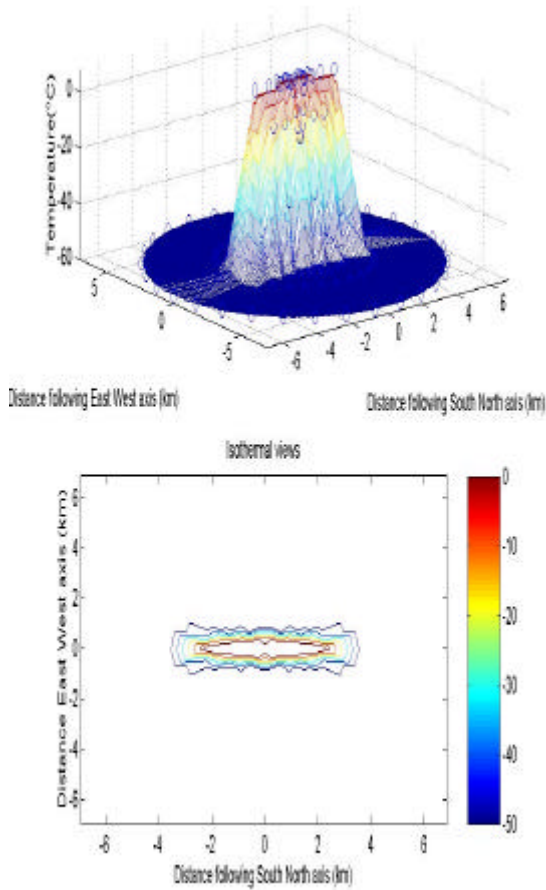Figure 4: *3D view and footprint for test # 2.*

Figure 5: *3D view and footprint for test # 5.*

Considering the low resolution these thermal footprints should be considered carefully.
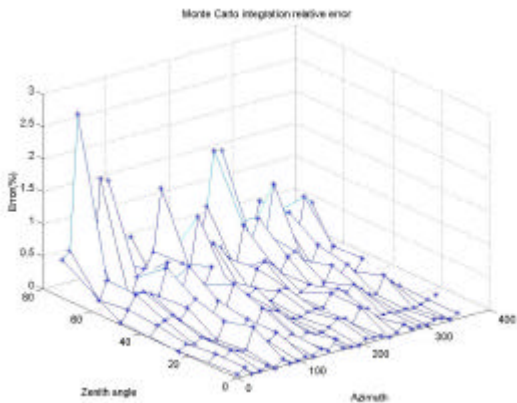

Figure 6: *Relative error on cloud surface.*

We studied also carefully the accuracy of the Monte Carlo integration for Nephelo and virtual cloud ellipses which are extremely weak even for configuration where the "shooting box has significant dimensions. Figure 6 and 7 show respectively accuracy for Nephelo ellipse and virtual cloud ellipse as a function of zenith angle

and azimuth. These figures show that, more important the zenith angle and the distance between the virtual cloud and the measurement ellipse are, more important the error percentage. This phenomenon is due to the size of the Monte Carlo "shooting box".
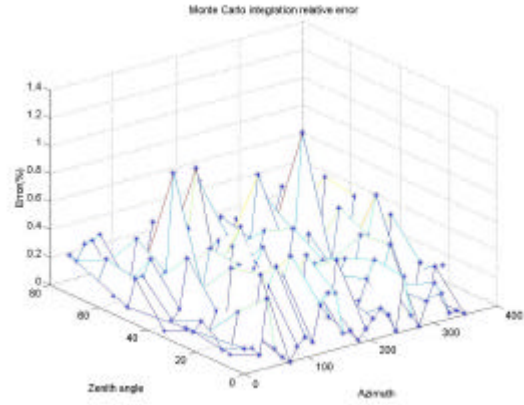

Figure 7: *Relative error on Nephelo ellipse surface.*

4. SECOND ORDER MOMENT METHOD FOR SHAPE CONSTRUCTION

4-1 METHOD DESCRIPTION

This method based on inertia moment (m_{nk}) calculation could be described as follow:

$$m_{nk} = \frac{1}{N} \sum_{i=1}^{181} P_i \left(x_i - x_G \right)^n \left(y_i - y_G \right)^k \quad \textbf{(2)}$$

where : - N is a normalization factor
- P is a weighting factor.
- (x_G, y_G) gravity center coordinates.

Summations above and below are performed on the 181 points of measurements provided by Nephelo.

After several tests, we defined N and P as follow:

$$P_i = S_i B \left(T_i \right)$$

$$N = \sum_{i=1}^{181} S_i B \left(T_i \right) \quad \textbf{(3)}$$

To take into account the overlap between the ellipses of measurement, as shown in figure 1, which is not a constant for the different ring-shaped areas of measurement, we redefined for each area 'measurement surfaces', **S$_i$,** as elementary elements of a radar diagram.

B(Ti) is a Boolean function of temperature. If the measurement ellipse of Nephelo receives no signal from the virtual cloud B(Ti) is equal to zero, and in the opposite case, equal to 1. We performed each computation considering two conditions:

T>-57°C (background temperature) (4)

T=T simulation (5)

P=S$_i$ B(T$_i$) (6)

Considering these formulas, we compute the following values: **m$_{20}$, m$_{02}$** and **m$_{11}$** by means of equations (7) to (9)

$$a = \sqrt{m_{02} + m_{20} + \sqrt{(m_{20} - m_{02})^2 + 4m_{11}^2}}$$
(7)

$$b = \sqrt{m_{02} + m_{20} - \sqrt{(m_{20} - m_{02})^2 + 4m_{11}^2}}$$
(8)

$$\mathbf{q} = \frac{1}{2}\arctan\left(\frac{2m_{11}}{m_{20} - m_{02}}\right)$$
(9)

where '**a**' is the inertia moment along the main axis of the shape, '**b**' the inertia moment perpendicular to a and '**theta**' the angle between 'a' and the horizontal axis.

4.2 SHAPE CONSTRUCTION vs. ALTITUDE

4.2.1 Simulations performed

We applied the method described in the previous paragraph to tests 1 to 7. Figures 8 and 9 show results of tests 2 and 5, respectively. On these figures black stars show measurement points at a temperature higher than the background temperature (-57°C) but lower than the simulation temperature, whereas blue stars measurement points are at the simulation temperature. Inside ellipse is built with the second order moment method with the points represented by blue stars and outside one using black and blue points.
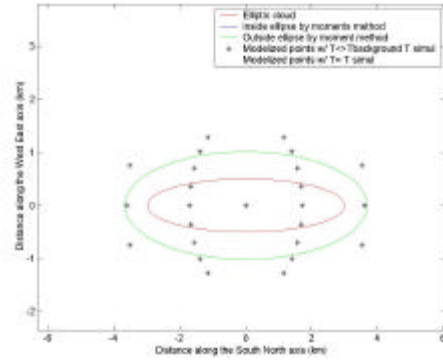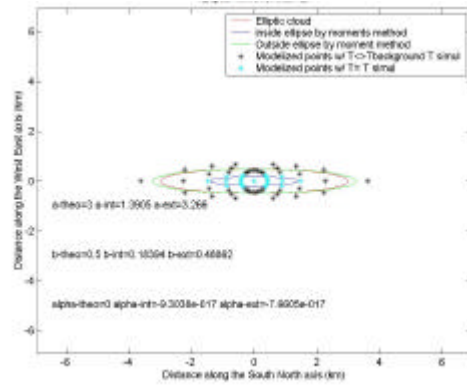

Figure 8: *Results for test # 2.*

Figure 9: *Results for test # 5.*

4-2-2 Results

• In the conditions of the simulations, the dimensions of the virtual cloud located at the zenith are relatively small (a=3 km b=0.5 km). Because the angular diameter of the cloud could be lower than the aperture of the sensor, the measured temperature could be thus significantly underestimated, i.e. at altitudes higher than 4500m in our previous example. This altitude limit will be smaller for clouds located in area with important values of zenith angle. We can say, in terms of field of applicability of this model that the altitude is strongly dependent on the size of the virtual cloud. Nevertheless, low altitude real clouds, and most of the mid-altitude clouds up to 4500-5000 m) could be simulated by his method, e.g. small Cumulus with ceiling high in the range of 2000 to 3000 m.

• As we can expect, globally inside ellipse underestimates the size of the shape and outside ellipse overestimates it. Due to the lack of resolution of the Nephelo "picture", a cut off temperature between −57 °C and temperature simulation does not provide any consistent optimization in the shape description. Usual interpolation methods (linear or spline) could be used. However, it is important to emphasise that

those methods have to be carefully controlled by means of cut away curves, as T versus distance.

• The second order moment method drove to accurate results concerning the angle of the main extension however about the description of the virtual cloud shape we looked for to obtain optimized results.

• Finally, notice that altitudes used in these simulations are generated by the MSISE-90 model that considers troposphere as an adiabatic media. Corrections could be introduced to simulate real cases.

4.3 SHAPE DESCRIPTION OPTIMIZATION

This method is based on an individual treatment of measurement ellipses partially overlapped by the virtual cloud (see black stars in figures 8 and 9) as they are at the limit of the shape.

For each ellipse, we analyzed the first neighborhood looking for location of fully overlapped measurement. To illustrate the method, an example based on a matrix of squares is presented in figure 10 (top).
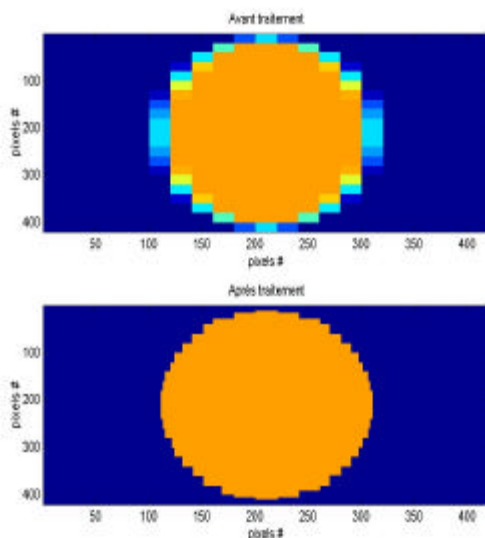

Figure 10: *Edge optimization, before (top) and after (bottom) treatment by the neighborhood method.*

Figure 10 (bottom) shows irregularities in the description of the shape that can be cleared by a single 'spline' process. However, we should keep in mind that the interface cloud/no cloud is not strict for most of cloud types except for 'congestus cumulus'.

4.4 TRUE CLOUDS TREATMENT

Previous sections described the different steps of the method design. For treatment of true situation it is necessary to proceed as following:

- Determination of an average minimum temperature that will be considered as background temperature. This step is due to the fact that "pure blue sky" is quite never observed in regular observation area. Cirrus and/or aerosols that are emitting in the thermal infrared wavelengths could generate this situation.

- Determination of the cloud cells number in the field of view of the instrument by means of a neighborhood process.

- Determination of cloud base temperature (ceiling).

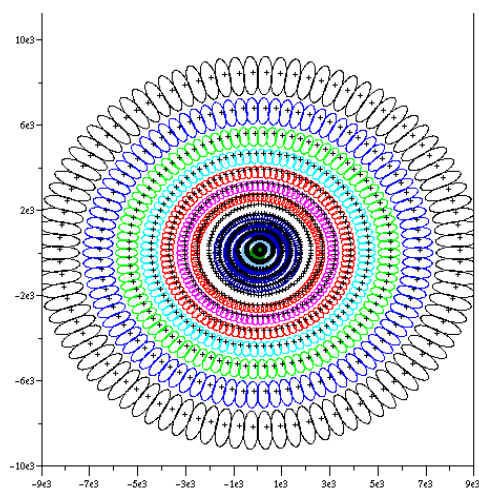- Picture re-construction with the methods described above

Figure 11: *Future grid of measurement of a Nephelo with 13 sensors.*

We will present pictures generated with the actual turret (7 pyrometers with a 12° interval and a stepping of 12°). We are at present optimizing the turret with a larger number of sensors providing an individual filed of view of 4° instead of 12° presently as shown in figure 11.

5. CONCLUSION

The 2-D simulations presented above permitted to optimize the cloud geometry reconstruction from the Nephelo measurements grid and to move from a 7 sensors to a 13 sensors configuration.

The virtual clouds simulations show that it was possible to detect, with a good accuracy, relatively small clouds (3 km x 0.5 km) at altitude up to 4.5 km. The neighborhood method allows also reconstructing the image of the virtual cloud despite the low resolution of the 7-sensor Nephelo.

This last aspect is of major interest for the treatment of the real clouds, by convoluting elementary ellipses, and the analysis of their water contents, with specific sensors, planned for the future development of the instrument.

6. ACKNOWLEDGMENTS

7. REFERENCES

Besnard T., D. Gillotay, G. Musquet, F. Zanghi and Y. Labaye, 2002: Mesures sol des formations nuageuses troposphériques par Spectrométrie infrarouge : Méthodologie, Intercomparaison et application in Proceedings of Atelier expérimentation et instrumentation, Toulouse, France.

Besnard T., D. Gillotay, F. Zanghi, W. Decuyper, C. Meunier and G. Musquet, 2002, Intercomparison of ground based methods for determination of tropospheric cloud base and cloud cover amplitude, in Proceedings of 11th conference on Atmospheric Radiation, Ogden, UT, USA, 3-7 June 2002.

Chernykh I.V., and R.E. Eskridge, 1996: Determination of cloud amount and level from radiosonde soundings. J. Appl. Meteor., **35**, 1362-1369.

Chernykh I.V., O.A. Alduchov and R.E. Eskridge, 2001: Trends in low and high clouds; Boundaries and Errors in height determination of cloud boundaries. Bull. Amer. Meteor. Society, **82**, 1941-1947.

Davies R. (2001) U. of Arizona, private communication .

Elskridge R. (2001) NCDC, private communication .

Gaumet J.L., N. Renoux, 1998: Cloud Cover Observations Using an IR sensor, in Proceedings of 10th symp. On Meteorological Observations and instrumentation, Phoenix, AZ, Amer. Meteor. Soc.,pp 161-164

Gillotay D., J.F. Müller, B. Walravens and P.C. Simon, 1997: The influence of different types of cloud layers on the UV climatology in Uccle, Belgium. in proceedings of the International Radiation Symposium '96: Current problems in atmospheric radiation, . Smith and Stamnes (eds.), pp 921-924.

Gillotay D., T. Besnard, F. Zanghi, 2001: A systematic approach of the cloud cover by thermic infrared measurements, in Proceedings of 18th conf. On weather analysis and forecasting – 14th conf. On numerical weather prediction. Fort Lauderdale, FL, Amer. Meteor. Soc., pp 292-295.

Gillotay D., T. Besnard and Y. Labaye, 2002, Impact of cloud spatial distribution on solar UV radiation transfer., in Proceedings of 11th conference on Cloud Physics, Ogden, UT, USA, 3-7 June 2002.

Hedin A.E., 1991, Extension of MSIS Thermospheric model into the middle and low atmosphere, J. Geophys. Res., **96,** 1159.

Labitzke K., J.J. Barnett and B. Edwards (eds.), 1985, Handbook MAP 16, SCOSTEP, University of Illinois, Urbana, USA .

WMO, 1996, in Guide to Meteorological Instruments and Methods of Observation, 6th Edition.